

# Free-standing microscale structures of nanocrystalline zirconia with biologically replicable three-dimensional shapes

Junping Zhao

*Department of Materials Science and Engineering, The Ohio State University, Columbus, Ohio 43210*

Christopher S. Gaddis, Ye Cai, and Kenneth H. Sandhage<sup>a)</sup>

*School of Materials Science and Engineering, Georgia Institute of Technology, Atlanta, Georgia 30332*

(Received 11 August 2004; accepted 1 November 2004)

Microscale zirconia structures with intricate three-dimensional (3D) shapes and nanoscale features were synthesized using diatom (single-celled algae) microshells as transient scaffolds. After exposure to a zirconium alkoxide-bearing solution and firing at 550–850 °C, silica-based diatom microshells were coated with a thin, continuous nanocrystalline zirconia layer. Predominantly tetragonal or monoclinic zirconia could be produced with appropriate heat treatments. Selective silica dissolution then yielded freestanding zirconia micro-assemblies that retained the microshell shape and fine features. Such hybrid (biological/synthetic chemical) processing may be used to mass-produce nanostructured micro-assemblies with a variety of 3D, biologically replicable shapes and tailored compositions for use in numerous applications.

Zirconia-based ceramics are technically important materials that are used, or considered for use, in a diverse range of applications such as oxygen sensors, oxygen pumps, electrochromic devices, fuel cells, thermal-barrier coatings, cutting tools, milling media, biomedical implants, ceramic membranes, and catalysts (e.g., isomerization of alkanes).<sup>1,2</sup> Nanocrystalline zirconia-based ceramics can exhibit enhanced catalytic, mechanical, thermal, and electrical properties.<sup>3–6</sup> The ability to mass-produce three-dimensional (3D) micro-assemblies of nanocrystalline zirconia would be highly attractive for a number of applications (e.g., for low-temperature gas sensing, minimally-invasive biomedical devices, rapid catalysis, and controlled-shape reinforcements in composites).<sup>1–6</sup> Appreciable global activity is underway to develop methods for assembling nanocrystal/nanoparticle-based structures with well-controlled chemistries, precise shapes, and fine features.<sup>7,8</sup> Processing approaches that can be scaled up for high-throughput production of 3D micro-assemblies on a massive (up to tonnage) scale, while retaining structural precision on a fine (down to nanometer) scale, are needed.

Numerous examples exist in nature of micro-organisms that, through sustained reproduction (repeated doubling), can assemble enormous numbers of microscale

biomineralized structures with well-controlled 3D shapes and meso-to-nanoscale features.<sup>9</sup> A particularly impressive range of such shaped bioclastic micro/nanostructures are generated by diatoms.<sup>10</sup> Diatoms are unicellular algae that populate a diverse range of aquatic environments (marine and freshwater; arctic to equatorial conditions).<sup>10</sup> Each diatom cell forms a rigid wall (frustule) consisting of a 3D microscopic assemblage of amorphous silica nanoparticles.<sup>10,11</sup> Each diatom species forms a uniquely shaped frustule with fine features (10<sup>2</sup> nm pores, ridges, protuberances, etc.) arrayed in intricate, species-specific patterns. Under appropriate conditions, diatom reproduction can occur several times per day, so that enormous numbers of similarly shaped frustules can be generated in a relatively short time<sup>10,12</sup> (e.g., at a sustained reproduction rate of 3 per day, 2<sup>30</sup> or more than 1 billion frustules of similar shape would be generated in 10 days, and more than 4 times Avogadro's number, 2<sup>81</sup> or 2.4 × 10<sup>24</sup>, would be produced in 27 days!). Such massively parallel and precise self-assembly of 3D nanoparticle structures under ambient conditions is highly attractive for nano-technological applications.<sup>13</sup> The estimated 10<sup>5</sup> extant diatom species also provide a diverse selection of frustule shapes and fine features for potential devices.<sup>10</sup> However, the use of diatom frustules in devices has been limited by the properties of silica. Attempts to introduce other oxides, such as germania, into diatom frustules during reproduction have yielded minimal changes in composition to date (e.g., only up to 0.02 wt% of <sup>68</sup>Ge, relative to <sup>31</sup>Si, was taken up in the

<sup>a)</sup>Address all correspondence to this author.

e-mail: ken.sandhage@mse.gatech.edu

DOI: 10.1557/JMR.2005.0046

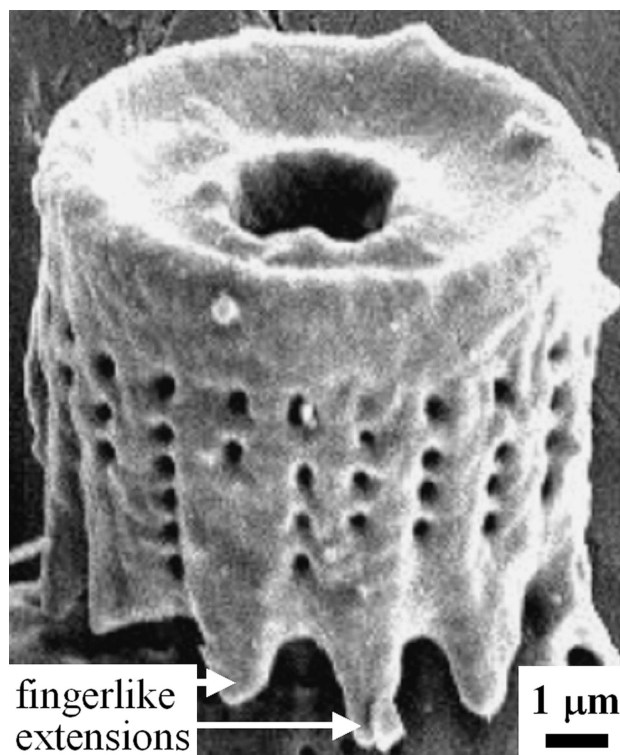
cell wall of *Nitzschia alba*<sup>14</sup>). Given the apparent inability of native diatoms to incorporate more than small amounts of oxides other than silica into their cell walls, alternate approaches are needed to significantly alter the frustule chemistry.

Gas/solid displacement reactions have recently been used to convert SiO<sub>2</sub>-based diatom frustules into MgO (via an oxidation-reduction reaction with magnesium gas)<sup>15</sup> or TiO<sub>2</sub> (via a metathetic reaction process involving titanium fluoride gas).<sup>16</sup> The magnesia and titania products of these displacement reactions retained the 3D shapes and fine (10<sup>2</sup> nm) features of the starting diatom frustules. However, the use of such gas/solid displacement reactions is limited to gaseous reactants that are capable of reducing silica or converting silica into a halide product.

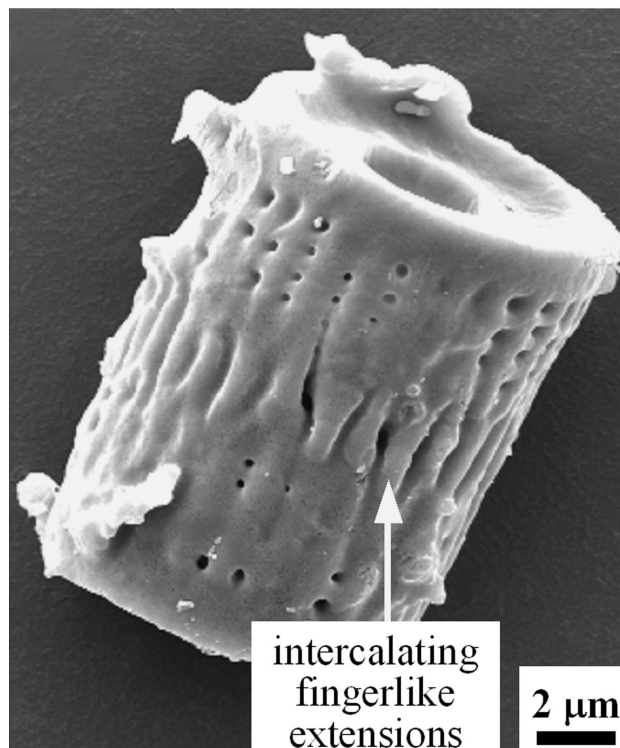
We demonstrate here, for the first time, how a wet chemical-based, ambient pressure (sol-gel) process may be used to completely convert silica-based diatom frustules into a new non-natural nanocrystalline ceramic compound (zirconia) while preserving the 3D frustule shape and fine features. Because this conversion process does not require a chemical reaction with silica to form the new compound, ceramic compositions may be accessed that would not be thermodynamically allowed with displacement reaction-based methods. Unlike prior work on the coating/filling of diatom frustules with siliceous zeolites,<sup>17</sup> the starting frustule scaffold is completely removed in the present process to yield silica-free ceramic structures that inherit the morphology (but not the chemistry) of the scaffold. The synthesis of a biologically shaped zirconia nanostructure is also a significant departure from recent work by Gaddis and Sandhage, who generated polymeric replicas of diatom frustules.<sup>18</sup> Although the fabrication and testing of a particular device is beyond the scope of this initial paper, the present work is a first step toward revealing how a combined biological and synthetic wet chemical process could be used to generate large numbers of controlled-shape, nanostructured ceramic assemblies with a wide range of non-silica-based chemistries for such devices.

In this work, the silica-based frustules of *Aulacoseira* diatoms were utilized as transient bioscaffolds for establishing the shapes of alkoxide-derived nanocrystalline zirconium oxide coatings. As revealed in Fig. 1, the *Aulacoseira* frustules were cylindrical in shape. The side walls of these frustules contained mesoscale pores (diameters of several hundred nanometers) arranged in rows running parallel to the cylinder length. One end face of each cylindrical frustule possessed a circular hole and a protruding outer rim [Fig. 1(a)]. The other end was closed with finger-like extensions. The fingerlike extensions from one cylinder intercalate with those of another to form a larger, paired assembly [Fig. 1(b)].

The *Aulacoseira* frustules were first immersed in a



(a)



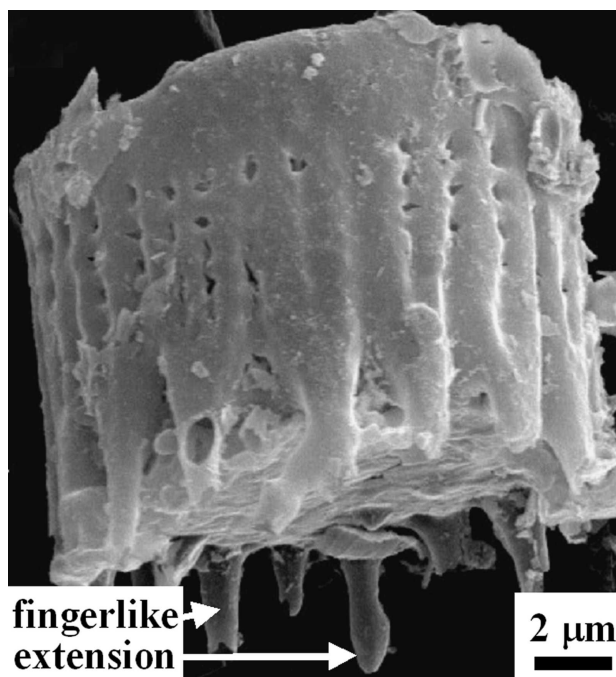
(b)

FIG. 1. Secondary electron images of silica-based *Aulacoseira* diatom frustules.

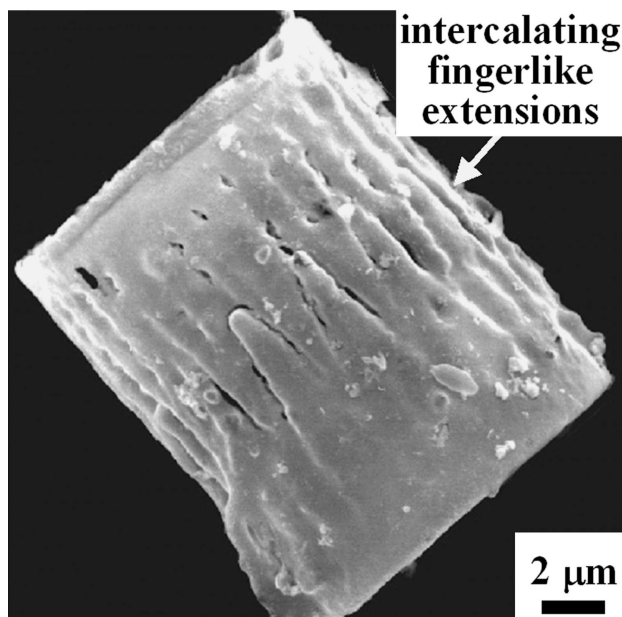
boiling ammonium hydroxide solution (pH = 10) for 4 h. After filtration from this solution and drying at room temperature, the frustules were exposed to a solution of zirconium n-propoxide (70 wt% in 1-propanol, Aldrich Chemical Co., Milwaukee, WI) with anhydrous ethanol, concentrated (29%) ammonium hydroxide, and de-ionized water (the solution possessed a molar  $\text{Zr}(\text{OC}_3\text{H}_7)_4$ :  $\text{NH}_4\text{OH}:\text{H}_2\text{O}:\text{EtOH}$  ratio of 1.0:0.67:3.36:480). Then 0.4 g hydrolyzed diatom frustules were added to 20 ml of this solution. The mixture was stirred and refluxed for 3 h at 76 °C. Eight milliliters of the solution were then allowed to evaporate at 66 °C. The mixture was stirred and refluxed for an additional hour, after which 5 ml more of the solution was allowed to evaporate. After conducting a final 2 h refluxing step, the solution was allowed to completely evaporate at 56 °C in air. After such complete evaporation (and a total of 6 h of refluxing), the coated frustules were collected and fired in air at a temperature in the range of 550–850 °C for 3 h. The silica in the zirconia-coated frustules was then selectively removed by immersion for 2 h in an aqueous 30 wt% sodium hydroxide solution at 85 °C.

Secondary electron images of the zirconia structures generated by the solution coating process after firing (650 °C for 3 h) and silica dissolution (NaOH solution) are shown in Fig. 2. These structures retained the cylindrical shapes and fine features of the starting silica-based frustules, which indicated that the zirconia coating was continuous and covered the entire frustule surface. The meso-scale pores on the side walls, and the fingerlike extensions on the closed ends of the frustules, were clearly preserved in the converted structures. An ion-milled cross-section obtained near the open end of a converted frustule is shown in Fig. 3(a) (note: although ion milling removed some of the protruding rim from the open end of this frustule, the hole at this end can still be clearly seen). This cross-section revealed that the continuous coating possessed a thickness of  $0.4 \pm 0.2 \mu\text{m}$ . Energy-dispersive x-ray analyses at various locations through this cross-section revealed distinct peaks for zirconium and oxygen [Fig. 3(b)] but not for silicon, which was consistent with complete removal of the silica by selective dissolution in the sodium hydroxide solution [note: the carbon peak was due to a carbon coating applied to the converted frustule to avoid electron beam charging in the scanning electron microscope (SEM)].

Room-temperature x-ray diffraction patterns obtained from the converted structures after firing at peak temperatures of 550, 650, or 850 °C for 3 h are shown in Figs. 4(a), 4(b), and 4(c), respectively. Residual crystalline silica (in the form of quartz, cristobalite, or tridymite) was not detected by x-ray diffraction analyses after any of these firing treatments. The predominant phase present after firing at 550 °C was tetragonal zirconia, with a small amount of monoclinic zirconia also



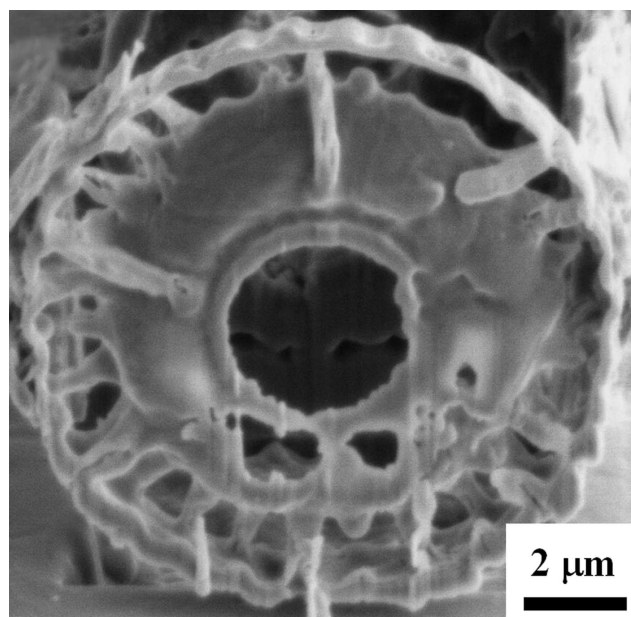
(a)



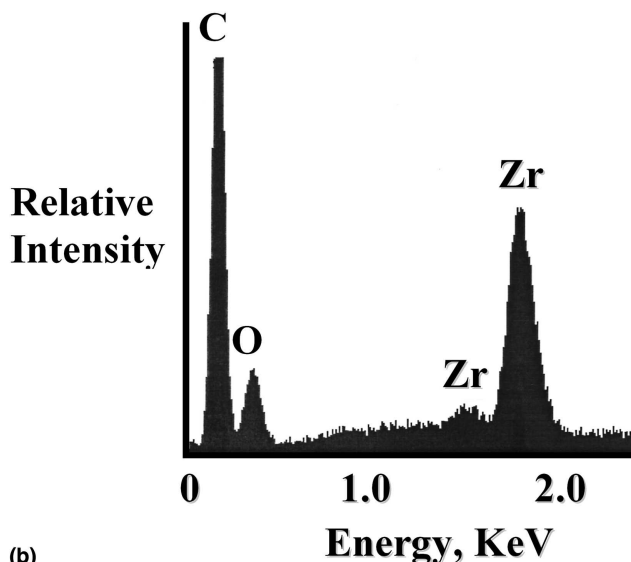
(b)

FIG. 2. Secondary electron images of free-standing zirconia structures generated from *Aulacoseira* diatoms, shown after silica removal with NaOH.

detected. With increasing firing temperature, the relative amounts of tetragonal and monoclinic zirconia decreased and increased, respectively. After the 850 °C treatment, monoclinic zirconia became the predominant phase. The observed conversion of tetragonal zirconia to monoclinic zirconia with increasing temperature is similar to that reported by other authors for sol-gel-derived zirconia



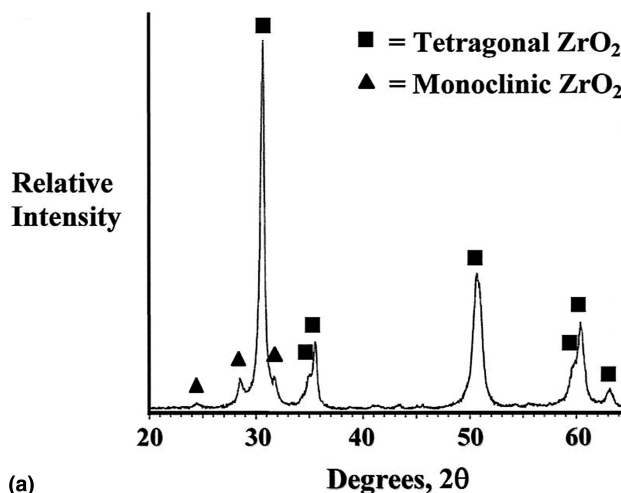
(a)



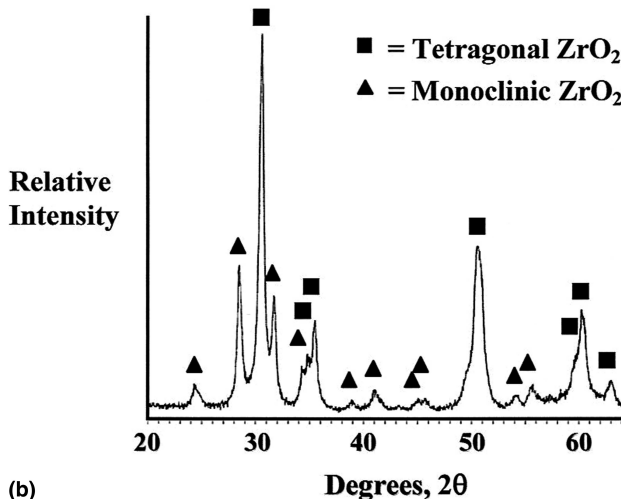
(b)

FIG. 3. (a) Secondary electron image of an ion-milled cross section of a zirconia-converted (silica-free) *Aulacoseira* frustule, and (b) an energy-dispersive x-ray analysis of the cross section.

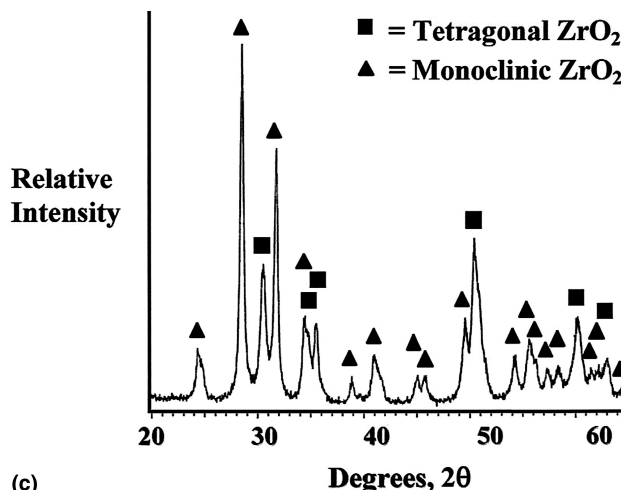
powders and zirconia films on fused silica.<sup>19,20</sup> The widths of the most intense diffraction peaks for tetragonal zirconia [the (101) peak near  $2\theta = 30$  degrees in Fig. 4(a)] and for monoclinic zirconia [the ( $\bar{1}11$ ) peak near  $2\theta = 28^\circ$  in Fig. 4(c)] were measured after the 550 and 850 °C heat treatments, respectively. Insertion of these values into the Scherrer equation yielded average crystallite sizes of 47 nm for tetragonal zirconia after 3 h at 550 °C and 42 nm for monoclinic zirconia after 3 h at 850 °C.<sup>21</sup> A dark-field transmission electron microscope (TEM) image confirming the nanocrystalline structure of a converted frustule is shown in Fig. 5(a). Electron diffraction



(a)



(b)



(c)

FIG. 4. X-ray powder diffraction analyses of zirconia-converted *Aulacoseira* frustules after firing in air for 3 h at (a) 550 °C, (b) 650 °C, and (c) 850 °C.

analysis of this specimen [Figs. 5(b) and 5(c)] revealed diffraction rings consistent with a mixture of tetragonal and monoclinic zirconia, in agreement with the x-ray diffraction analysis in Fig. 4(b).

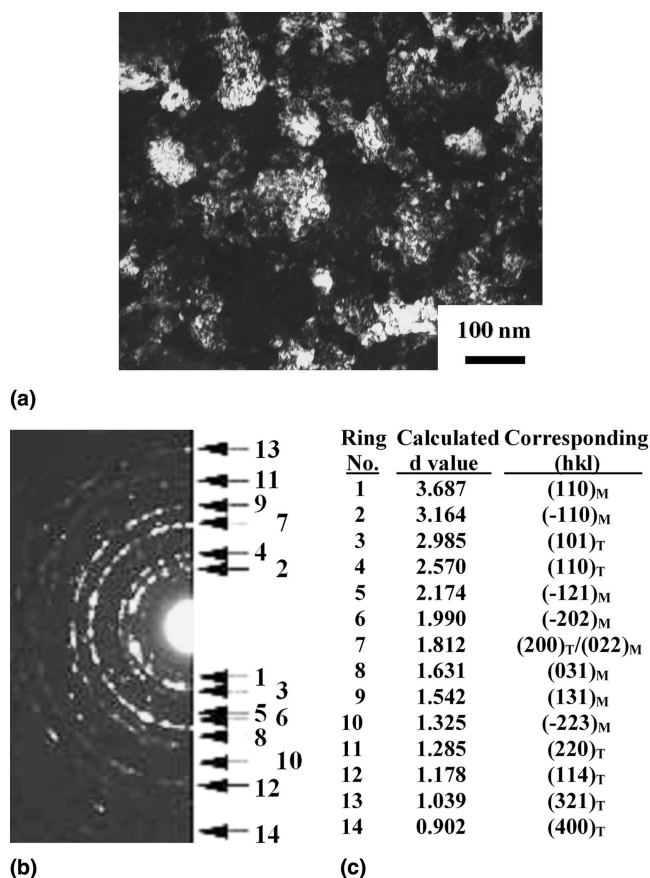


FIG. 5. (a) Dark-field TEM image and (b) electron diffraction pattern obtained from an ion-milled cross-section of a zirconia-converted frustule after firing for 3 h at 650 °C. Calculated  $d$  spacings from diffraction rings 1–14 and associated  $hkl$  values for monoclinic and tetragonal zirconia are shown in (c).

A layer of zirconia on silica is not thermodynamically stable; that is, the compound zircon ( $ZrSiO_4$ ) should eventually form by the reaction of the zirconia layer with the underlying silica. However, the free-standing structures shown in Figs. 2 and 3 were free of zircon, as deduced by energy dispersive x-ray analyses in the SEM and TEM (i.e., silicon was not detected), x-ray diffraction analyses, and electron diffraction analyses of specimen cross-sections in the TEM. The absence of zircon was likely due to the slow rate of zircon formation from zirconia and silica at 550–850 °C. Indeed, several authors have reported that such zircon formation is quite sluggish at temperatures below 1200 °C.<sup>22,23</sup>

The present work provides the first demonstration that a wet chemical, ambient pressure (sol-gel) approach can be used to completely convert a 3D nanoparticle structure assembled by a self-replicating micro-organism into a new nanocrystalline, non-biogenic-based ceramic compound without a loss of shape or fine (submicron) features. Such shape-preserving chemical conversion enables bioclastic structures to be endowed with a much

broader range of properties than are exhibited by biogenic amorphous silica or calcium carbonate (the most common mineral compositions for bioclastic structures<sup>9</sup>). Indeed, relative to amorphous silica or calcite, zirconia-based compositions can possess significantly enhanced catalytic activity, ionic and electronic conductivity, hardness and toughness, and high-temperature stability in oxidizing environments.<sup>1–6</sup> Furthermore, because a wide variety of functional coatings can be produced from alkoxide and other synthetic precursors, this process may be used to convert diatom frustules into a host of other chemically tailored nanocrystalline assemblies with attractive electronic, magnetic, optical, chemical, biochemical, or mechanical properties. As mentioned earlier, a wide variety of natural frustule shapes are available for selection as bioscaffolds. Future developments in genetic engineering could be used to produce an even greater range of tailored shapes and fine features. Indeed, initial steps have been taken in this direction. Transformation-based approaches have been developed for introducing and expressing genes in diatoms, and a diatom genome (*Thalassiosira pseudonana*) has recently been sequenced.<sup>24–26</sup> The present process may also be applied to bioclastic micro-assemblies generated by numerous other types of algae, bacteria, fungi, or other microorganisms.<sup>9</sup> The self-replicating nature of such bioscaffolds enables enormous numbers of nanocrystalline structures with similar, well-controlled 3D shapes, fine features, and tailored chemistries to be produced. The multifarious combinations of natural or genetically modified bioclastic shapes and synthetic chemistries that may be utilized in this hybrid process could yield a diverse spectrum of microdevices (sensors, filters, membranes, reactors, transducers, capsules, etc.) for transportation, environmental, biomedical, petrochemical, energy production and storage, and defense applications.<sup>1–6,13</sup>

## ACKNOWLEDGMENT

This work was supported by the Air Force Office of Scientific Research (Dr. Joan Fuller and Dr. Hugh DeLong, Program Managers).

## REFERENCES

1. I. Birkby and R. Stevens: Applications of zirconia ceramics. *Key Eng. Mater.* **122**, 527 (1996).
2. B. Li and R.D. Gonzalez: Sol-gel synthesis and catalytic properties of sulfated zirconia catalysts. *Ind. Eng. Chem. Res.* **35**, 3141 (1996).
3. A.V. Shevchenko, E.V. Dudnik, A.K. Ruban, V.P. Red'ko, V.M. Vereschaka, and L.M. Lopato: Nanocrystalline powders based on  $ZrO_2$  for biomedical applications and power engineering. *Powder Metall. Met. Ceram.* **41**, 558 (2002).
4. O. Vasylyuk, Y. Sakka, and V.V. Skorokhod: Low-temperature processing and mechanical properties of zirconia and zirconia-alumina nanoceramics. *J. Am. Ceram. Soc.* **86**, 299 (2003).

5. M. Boaro, A. Trovarelli, J-H. Hwang, and T.O. Mason: Electrical and oxygen storage/release properties of nano-crystalline ceria-zirconia solid solutions. *Solid State Ionics* **147**, 85 (2002).
6. G. Soyez, J.A. Eastman, L.J. Thompson, G-R. Bai, P.M. Baldo, A.W. McCormick, R.J. DiMelfi, A.A. Elmustafa, M.F. Tambwe, and D.S. Stone: Grain-size-dependent thermal conductivity of nanocrystalline yttria-stabilized zirconia films grown by metal-organic chemical vapor deposition. *Appl. Phys. Lett.* **77**, 1155 (2000).
7. J.J. Storhoff, R.C. Mucic, and C.A. Mirkin: Strategies for organizing nanoparticles into aggregate structures and functional materials. *J. Cluster Sci.* **8**, 179 (1997).
8. E. Rabani, D.R. Reichman, P.L. Geissler, and L.E. Brus: Drying-mediated self-assembly of nanoparticles. *Nature* **426**, 271 (2003).
9. H.A. Lowenstam and S. Weiner: Mineralization by organisms and the evolution of biomineralization, in *Biomineralization and Biological Metal Accumulation*, edited by P. Westbroek and E.W. de Jong (D. Reidel Publishing Co., Dordrecht, Holland, 1983), p. 191.
10. F.E. Round, R.M. Crawford, and D.G. Mann: *The Diatoms: Biology & Morphology of the Genera* (Cambridge University Press, Cambridge, U.K., 1990).
11. S.A. Crawford, M.J. Higgins, P. Mulvaney, and R. Wetherbee: Nanostructure of the diatom frustule as revealed by atomic force and electron microscopy. *J. Phycol.* **37**, 543 (2001).
12. T. Lebeau and J-M. Robert: Diatom cultivation and biotechnologically relevant products. Part I: Cultivation at various scales. *Appl. Microbiol. Biotechnol.* **60**, 612 (2003).
13. J. Parkinson and R. Gordon: Beyond micromachining: The potential of diatoms. *Trends Biotechnol.* **17**, 190 (1999).
14. C.W. Mehard, C.W. Sullivan, F. Azam, and B.E. Volcani: Role of silicon in diatom metabolism. IV. Subcellular localization of silicon and germanium in *Nitzschia alba* and *Cylindrotheca fusiformis*. *Physiol. Plant.* **30**, 265 (1974).
15. K.H. Sandhage, M.B. Dickerson, P.M. Huseman, M.A. Caranna, J.D. Clifton, T.A. Bull, T.J. Heibel, W.R. Overton, and M.E.A. Schoenwaelder: Novel, bioclastic route to self-assembled, 3D, chemically tailored meso/nanostructures: shape-preserving reactive conversion of biosilica (diatom) microshells. *Adv. Mater.* **14**, 429 (2002).
16. R.R. Unocic, F.M. Zalar, P.M. Sarosi, Y. Cai, and K.H. Sandhage: Anatase assemblies from algae: Coupling biological self-assembly of 3-D nanoparticle structures with synthetic reaction chemistry. *Chem. Comm.* **7**, 795 (2004).
17. M.W. Anderson, S.M. Holmes, N. Hanif, and C.S. Cundy: Hierarchical pore structures through diatom zeolitization. *Angew. Chem. Int. Ed. Engl.* **39**, 2707 (2000).
18. C.S. Gaddis and K.H. Sandhage: Freestanding microscale 3-D polymeric structures with biologically-derived shapes and nanoscale features. *J. Mater. Res.* **19**, 2541 (2004).
19. J.A. Wang, M.A. Valenzuela, J. Salmones, A. Vazquez, A. Garcia-Ruiz, and X. Bokhimi: Comparative study of nanocrystalline zirconia prepared by precipitation and sol-gel methods. *Catal. Today* **68**, 21 (2001).
20. H. Li, K. Liang, S. Gu, and G. Xiao: Oriented nanostructured  $ZrO_2$  thin films on fused quartz substrate by sol-gel process. *J. Mater. Sci. Lett.* **20**, 1301 (2001).
21. B.D. Cullity: *Elements of X-ray Diffraction* (Addison-Wesley Publishing Co., Reading, MA, 1978), p. 101.
22. Y. Kanno: Thermodynamic and crystallographic discussion of the formation and dissociation of zircon. *J. Mater. Sci.* **24**, 2415 (1989).
23. T. Itoh: Zircon ceramics prepared from hydrous zirconia and amorphous silica. *J. Mater. Sci. Lett.* **13**, 1661 (1994).
24. T.G. Dunahay, E.E. Jarvis, and P.G. Roessler: Genetic transformation of the diatoms *Cyclotella Cryptica* and *Navicula Saprophylla*. *J. Phycol.* **31**, 1004 (1995).
25. L.A. Zaslavskaja, J.C. Lippmeier, P.G. Kroth, A.R. Grossman, and K.E. Apt: Transformation of the diatom *Phaeodactylum Tricornutum* (Bacillariophyceae) with a variety of selectable marker and reporter genes. *J. Phycol.* **36**, 379 (2000).
26. Web site of the Joint Genome Institute: U.S. Department of Energy: <http://genome.jgi-psf.org/thaps1/thaps1.home.html>